Jurnal Kejuruteraan 37(3) 2025: 1563-1570
https://doi.org/10.17576/jkukm-2025-37(3)-37

Evaluation and Computational Modelling of Planar Electrolyte-Supported SOFC

Ole Ronie[a,b*], Wan Aizon W. Ghopa[a], Nurul Akidah Baharuddin[b], Mahendra Rao Somalu[c], Noor Shieela Kalib[d] & Andanastuti Muchtar[a]

[a]*Department of Mechanical and Manufacturing Engineering,*
Faculty of Engineering & Built Environment, Universiti Kebangsaan Malaysia, Malaysia.

[b]*Fuel Cell Institute, Research Complex, Universiti Kebangsaan Malaysia.*

[c]*Lynas Malaysia Sdn. Bhd., PT 17212, Jalan Gebeng 3,*
Kawasan Perindustrian Gebeng, 26080 Kuantan Pahang Darul Makmur, Malaysia.

[d]*School of Engineering & Physical Science-Mechanical,*
Heriot-Watt University, 62200 Putrajaya, Malaysia

[*]*Corresponding author: oleroniewayne@gmail.com*

Received 30 June 2024, Received in revised form 10 February 2025
Accepted 10 March 2025, Available online 30 May 2025

ABSTRACT

Solid Oxide Fuel Cells (SOFCs) are a cutting-edge technology for converting chemical energy into electrical energy, offering exceptional efficiency and compatibility with renewable energy systems, making them integral to sustainable energy solutions. This study addresses a specific gap in the research of single-channel planar electrolyte-supported SOFC models, which face challenges in achieving accurate simulations through computational fluid dynamics (CFD) due to limited studies and inherent modelling complexities. The primary objective of this work is to develop and validate planar electrolyte-supported model using advanced CFD techniques. A comprehensive grid independence test was conducted, confirming the reliability of the simulation with the current output stabilizing at 121,176 elements with 0.73V. Further analysis revealed that reducing the node distance along the y-axis (reaction direction axis) significantly influenced the current output, showing variations of 19-21% percentage difference, compared to less than 5% along the x-axis (perpendicular direction to fuel direction axis) and z-axis (fuel direction axis). To enhance the model's reliability, its results were validated against findings from other studies using different SOFC design model and criteria but sharing similar concepts, with comparisons incorporating both simulation and experimental data. These validations confirmed the model's high accuracy and reliability. The findings establish planar electrolyte-supported SOFC model as a reliable and valuable design for advancing research, enabling performance optimization, and addressing the challenges of sustainable energy technologies. Furthermore, by considering time and cost, this simulation study can be a reference in predicting the performance of future SOFC research.

Keywords: Solid oxide fuel cell; planar electrolyte-supported; modelling; computational fluid dynamics; grid independence test

INTRODUCTION

Global climate change concerns and the ongoing energy crisis are stimulating the demand for renewable energy solutions with zero or even negative emissions (He et al. 2023). Around the world national governments are responding by committing to transformational new clean energy technologies through the energy revolution itself. As one of the most promising technologies for sustainable energy, the hydrogen economy has become an important solution that encompasses the production, storage, and conversion of hydrogen to usable energy (Aznam et al. 2023; Pang et al. 2024). In this scenario, Solid Oxide Fuel Cells (SOFCs) have attracted considerable attention due to their high efficiency, enhanced waste heat recovery, and fuel flexibility. Moreover, SOFC are capable of using multiple fuels including hydrogen, natural gas, bio-ethanol, and other hydrocarbons, thus minimizing the demand for

complicated and expensive fueling infrastructure (Khanafer et al. 2022). These traits make SOFCs a key technology for enabling large scale renewable energy over the next few decades. However, the high operating temperature causes degradation of SOFC; thus, efforts to reduce the temperature of SOFC are being researched (Mah et al. 2023).

Planar Electrolyte Supported SOFCs are scalable and cost-effective but suffer from high ohmic losses due to their thick electrolyte (>200 µm), reducing efficiency compared to other SOFC types (Mathur et al. 2023). Anode-supported SOFCs, with a thinner electrolyte (~10–20 µm), minimize ohmic losses and offer better performance at lower temperatures. Cathode-supported SOFCs, though less common, face limitations due to slow oxygen reduction kinetics. Metal-supported SOFCs provide mechanical strength and rapid thermal cycling but require complex fabrication. Unlike these alternatives, electrolyte-supported SOFCs are simpler to manufacture but operate at higher temperatures, leading to longer start-up times and material degradation (Singh et al. 2021).

Recent studies been concentrated on the factors effecting the electrical performance of SOFC including tortuosity in the porous materials of the electrodes. It has been found that tortuosity reduction improves SOFCs ionic and electrical conductivity and performance. Many of these works focus on the modeling of single-channel anode-supported SOFCs directly fed hydrogen or water vapor, mainly with the help of planar configurations and computation tools (Zhang et al. 2021). Moreover, computational fluid dynamics (CFD) methods are commonly used to investigate flow behavior and gas distribution in SOFC stacks, which can provide crucial information to improve the performance of SOFCs (Chen et al. 2023). These computational models play a critical role in progressing the design and efficiency of SOFC systems and in giving insights in internal processes such as heat and mass transfer. There is little information available on the performance of biogas-fueled single-channel SOFC systems, and hence the present study focuses on developing and verifying a model for this type of electrolyte-supported SOFC.

Similar studies have explored the performance of anode-supported SOFCs fueled by biogas, using CFD software like ANSYS and COMSOL to model their behavior and efficiency (Mehrabian & Mahmoudimehr 2023; Nouri et al. 2024). However, due to lack of research in planar electrolyte-supported, this study aims to develop and evaluate a model for a planar electrolyte-supported SOFC. This objective is pursued through CFD analysis, including a grid independence test and model validation, to ensure accurate and reliable performance predictions.

METHODOLOGY

MODEL AND MATERIALS

The study employs a planar electrolyte-supported solid oxide fuel cell (SOFC) single-channel cell model. This model comprises several key components: the anode, cathode, electrolyte, and channels. The anode is constructed from Ni-Cu-ScCeSZ (Nickel-Copper-Scandium-Cerium Stabilized Zirconia), while the cathode is made of LSCF-ScCeSZ (Lanthanum Strontium Cobalt Ferrite-Scandium Cerium Stabilized Zirconia). The electrolyte, which is crucial for ion conduction, consists of ScCeSZ (Scandium Cerium Stabilized Zirconia) (Arifin et al. 2023; Lee et al. 2022; Mohd Abd Fatah et al. 2022; Muhammed Ali Shaikh Abdul Kader Abdul et al. 2022; Pongratz et al. 2022; Zainon et al. 2023). The model includes distinct fuel and air channels, with interconnects facilitating the flow of gases and electrons (Shieela Kalib et al. 2022). Figure 1 shows the dimension used for the model for simulation.

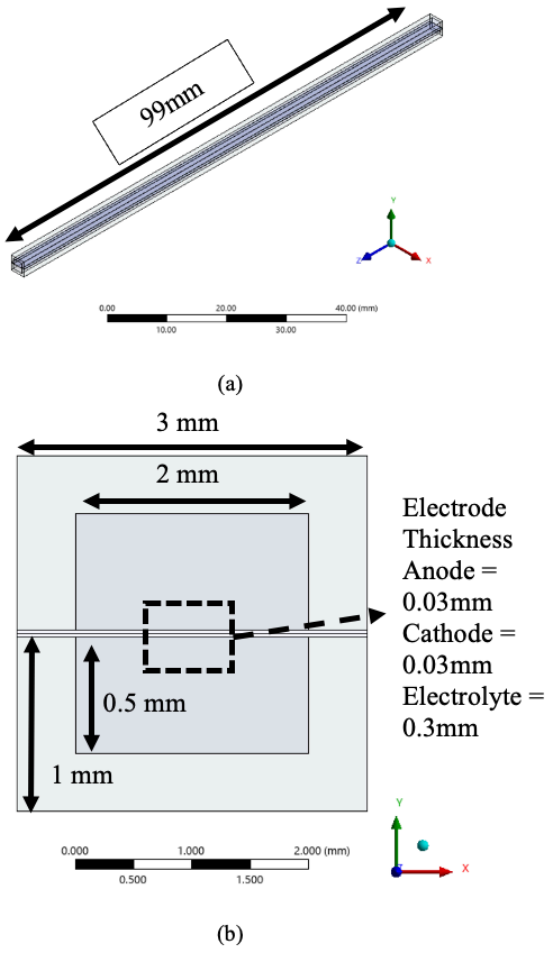

FIGURE 1. Model with Dimension (a) Isometric View and (b) Front View

For the simulation, ANSYS Fluent with the SOFC add-on module was utilized. This software is capable of solving various critical equations, including those related to fluid flow, mass transfer, heat transfer, reactions, and the transport of current and potential fields. This comprehensive computational approach allows for a detailed analysis of the cell's performance under different conditions.

ASSUMPTION AND BOUNDARY CONDITION

In this simulation, several fundamental assumptions were made to simplify the modeling process while ensuring accuracy in representing the physical and chemical phenomena occurring within the solid oxide fuel cell (SOFC). Firstly, the gas behavior was assumed to follow the ideal gas law, which allows for straightforward calculations of thermodynamic properties without considering intermolecular interactions. Secondly, the flow regime within the cell was treated as laminar and incompressible due to the relatively low Reynolds number characteristic of SOFC operation. This assumption ensures that turbulence modeling is not required, simplifying the computational complexity. Thirdly, the chemical reactions were considered to occur under steady-state conditions, implying that transient effects such as time-dependent concentration variations were neglected. Additionally, radiation heat transfer was assumed negligible compared to conduction and convection, given that the primary mode of heat transfer within the SOFC occurs via solid conduction and convective gas transport. Lastly, it was assumed that the gases flow smoothly from the inlet to the outlet and diffuse through the porous electrode structure, enabling uniform reactant distribution and realistic mass transport modeling (Mehrabian & Mahmoudimehr 2023; Nouri et al. 2024)

The boundary conditions were carefully defined to establish a comprehensive and realistic operational environment for the SOFC model. The fuel and air channels were configured in a counter-flow arrangement, which enhances thermal efficiency by optimizing temperature gradients across the cell. The model included two interconnects, one for the anode and another for the cathode, which function as electrical and gas distribution components. The cell was operated at a base temperature of 700°C, a standard condition for intermediate-temperature SOFCs, which balances performance and material stability. Furthermore, the system pressure was set at atmospheric pressure (101,325 Pa or 1 atm), simplifying the calculations while reflecting practical operating conditions. The primary fuel mixture consisted of methane (CH_4) and carbon dioxide (CO_2), commonly found in biogas and syngas applications, which supports internal reforming processes within the SOFC.

To accurately model the electrochemical and thermochemical processes in the fuel cell, key reforming reactions were incorporated. These included methane steam reforming ($CH_4 + H_2O \rightleftharpoons CO + 3H_2$), which produces hydrogen as the primary fuel for the electrochemical reactions at the anode. Additionally, the water-gas shift reaction ($CO + H_2O \rightleftharpoons CO_2 + H_2$) was considered, as it further enhances hydrogen production while regulating the carbon monoxide concentration. Lastly, the reverse water-gas shift reaction ($CO_2 + H_2 \rightleftharpoons CO + H_2O$) was included to account for equilibrium effects that influence syngas composition within the anode chamber. These reactions, combined with the specified assumptions and boundary conditions, create a robust framework for evaluating the performance and efficiency of the SOFC under simulated operating conditions.

GRID INDEPENDENCE TEST

The grid independence test was performed using ANSYS Mesh to ensure that the simulation results were not significantly influenced by the mesh resolution. This was achieved by systematically refining the mesh along the x-axis, y-axis, and z-axis, thereby adjusting the number of elements and nodes within the computational domain. The primary goal of this process was to identify an optimal mesh density that provided accurate and stable results while minimizing computational cost. To achieve this, multiple simulations were conducted with progressively finer meshes, and the key performance parameters were compared across different grid resolutions. The results were considered grid-independent when the percentage difference between successive simulations fell within an acceptable threshold of 5% or less. This approach ensured that the selected mesh resolution was sufficient to capture the necessary physical and chemical phenomena without excessive computational burden, ultimately balancing accuracy and efficiency in the simulation process.

The percentage difference can be calculated using Equation (1), where δ% is the percentage difference, v_a is the actual current obtained from the number of elements, and v_e is the expected current

$$\delta\% = \left|\frac{v_a - v_e}{v_e}\right| x100\% \quad (1)$$

Using Equation (1), Figure 2 was obtained which shows the relationship between the current and the number of elements.

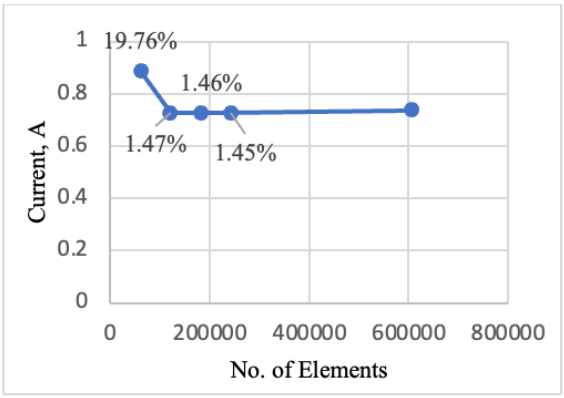

FIGURE 2. Grid Independence Test

As depicted in the figure, the initial mesh with 60,588 elements resulted in a percentage difference of 19.76%, which is significantly higher than the acceptable threshold of 5%. By increasing the number of elements to 121,176, the percentage difference was reduced to 1.47%, falling well within the acceptable range. Further increases in the number of elements, such as 181,764, 242,352, and 484,040, did not result in significant decreases in the percentage difference, which remained around 1.45%-1.46%

Therefore, the mesh with 121,176 elements was chosen for the simulation, as it provided accurate and consistent results while maintaining computational efficiency. This balance ensured that the simulation could be conducted within a reasonable timeframe without compromising the accuracy of the results

VALIDATION

The validation was conducted by comparing the results of this study with those of (Ghorbani & Vijayaraghavan 2018) and (Tikiz et al. 2019), who used the same fuel but different boundary conditions, assumptions, material properties, and model dimensions. The figure shows a similar downward trend where the voltage decreases as the current increases. However, the model used by Ghorbani & Vijayaraghavan 2018 exhibits a complete drop to 0 V at approximately 1.4 A, likely indicating that their model had reached its maximum potential.

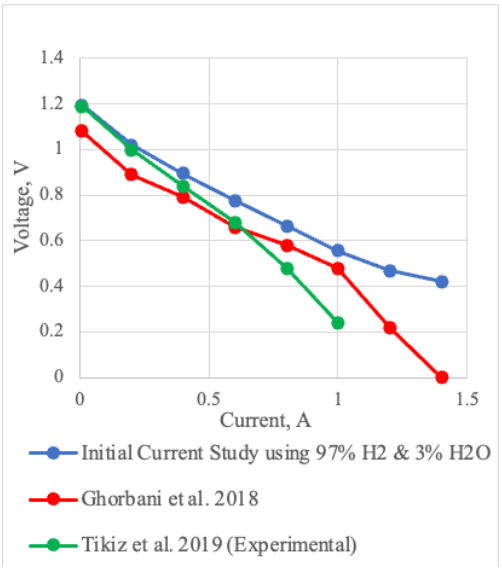

FIGURE 3. Validation with Past Research

In contrast, the model used in this study continues to produce voltage as the current increases, demonstrating its potential to maximize performance output for further study. This sustained voltage suggests that the model can be optimized further to enhance its efficiency and performance, making it a promising candidate for future research and development in SOFC technology

RESULT AND DISCUSSION

Table 1 presents the meshing parameters and corresponding current (I) values, along with their percentage differences for various configurations of a simulation model. The parameters include the number of elements, the sizes of the x-, y-, and z-axes, the resulting current, and the percentage difference from a reference or optimal value.

TABLE 1. Effect of X, Y and Z-Axis of Edge Sizing on Current Output

No. of Elements	X	Y	Z	Current
60588	5.00E-04	3.00E-05	1.00E-03	0.886
121176	2.50E-04	3.00E-05	1.00E-03	0.894
181764	1.67E-04	3.00E-05	1.00E-03	0.897
242352	1.25E-04	3.00E-05	1.00E-03	0.898
302940	1.00E-04	3.00E-05	1.00E-03	0.899

continue ...

... cont.

121176	5.00E-04	1.50E-05	1.00E-03	0.729
242352	2.50E-04	1.50E-05	1.00E-03	0.735
363528	1.67E-04	1.50E-05	1.00E-03	0.737
484704	1.25E-04	1.50E-05	1.00E-03	0.737
605880	1.00E-04	1.50E-05	1.00E-03	0.738
181764	5.00E-04	1.00E-05	1.00E-03	0.729
363528	2.50E-04	1.00E-05	1.00E-03	0.735
545292	1.67E-04	1.00E-05	1.00E-03	0.737
727056	1.25E-04	1.00E-05	1.00E-03	0.735
908820	1.00E-04	1.00E-05	1.00E-03	0.736
242352	5.00E-04	7.50E-06	1.00E-03	0.729
484704	2.50E-04	7.50E-06	1.00E-03	0.735
727056	1.67E-04	7.50E-06	1.00E-03	0.735
969408	1.25E-04	7.50E-06	1.00E-03	0.735
1211760	1.00E-04	7.50E-06	1.00E-03	0.734

The data shows that while increasing the number of elements generally aims to improve accuracy, the y-axis size plays a particularly significant role in influencing the results. Configurations with a larger y-axis size of 3.00E-05 exhibit high percentage differences, often above 20%. However, when the y-axis size is reduced to 1.50E-05 or smaller, the percentage differences in current values decrease significantly, frequently falling below the 5% threshold.

For instance, with an element count of 121,176 and a y-axis size of 1.50E-05, the percentage difference is 1.472%, whereas the same element counts with a y-axis size of 3.00E-05 shows a much higher percentage difference of 20.855%. Similarly, with 242,352 elements and a y-axis size of 7.50E-06, the percentage difference is only 1.455%. This trend continues with higher element counts, where finer y-axis meshes yield low percentage differences, indicating improved accuracy. For example, at 605,880 elements with a y-axis of 1.50E-05, the percentage difference is as low as 0.293%.

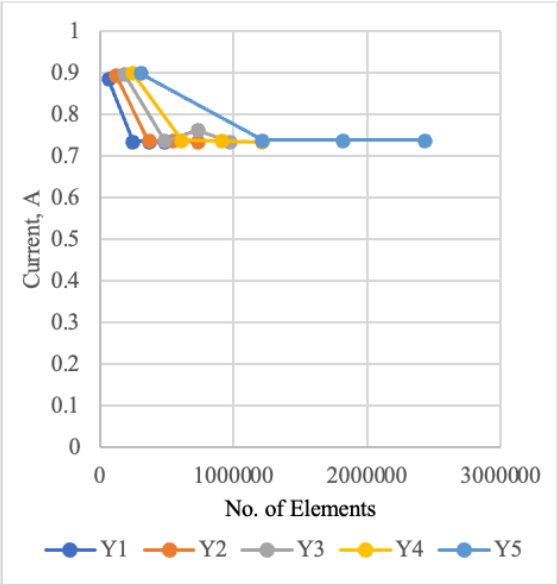

FIGURE 5. Effect of Edge Sizing of Y-Axis (Reaction Direction)

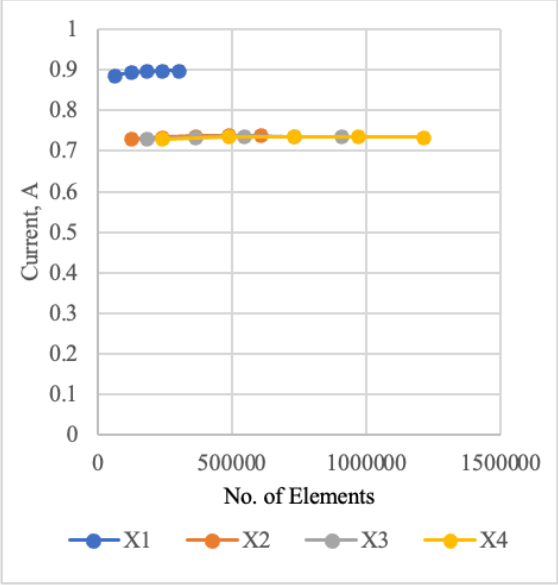

FIGURE 6. Effect of Edge Sizing of X-Axis (Perpendicular to Z-Axis)

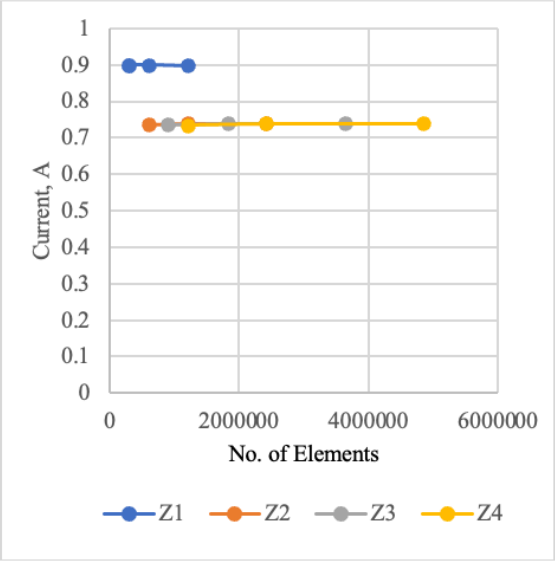

FIGURE 7. Effect of Edge Sizing of Z-Axis (Flow Direction)

For Figure 5, the graph is plotted with a constant z-axis and y-axis. When the x-axis is reduced from 5E-004 to 1E-004, the results remain consistent within a 5% percentage difference, falling within the range of 0.8–0.9 A. However, when the y-axis is reduced from 3E-005 to 1.5E-005, the current output decreases to a range of 0.72–0.74 A. The x-axis was then reduced in the same manner, from 5E-004 to 1E-004, but the results remained in the same range. Therefore, Figure 6 was plotted to further investigate the y-axis behavior.

Figure 6 illustrates the effects when the x-axis and z-axis are held constant. When the y-axis is reduced from 3E-005 to 7.5E-006, the results show a significant percentage difference between 3E-005 and 1.5E-005, with the current output dropping from the 0.8–0.9 A range to the 0.72–0.74 A range. When the y-axis is further reduced from 1.5E-005 to 1E-005 and then to 7.5E-006, the current output shows little to no changes, with differences below 5%. This demonstrates that meshing along the y-axis has a significant impact on the performance and accuracy of the results.

Figure 7 was plotted with the x-axis and y-axis held constant. When the z-axis was reduced from 1E-003 to 5E-004 and then to 2.5E-004, there was only a very small change in performance in terms of current output. This indicates that the z-axis has minimal contribution to the accuracy of the model.

The findings from this study highlight the critical influence of y-axis meshing on the accuracy of CFD simulations for SOFCs. While increasing the number of elements generally improves accuracy, the results show that refining the y-axis mesh size has a far more significant impact on reducing percentage differences in current output. When the y-axis is reduced from 3.00E-05 to 1.50E-05 or smaller, the percentage differences drop considerably, frequently falling below 5% compared to other current output values. Additionally, further reductions beyond 1.50E-05 show minimal impact on the current output, indicating that the mesh has reached its optimal resolution at 1.50E-05. In contrast, refining the x-axis and z-axis has minimal impact on accuracy, suggesting that mesh refinement along these axes is less critical. Although the fuel and air flow in the z-axis direction, the rate of reaction determines the current output. This aligns with the reaction direction, as reactions primarily occur along the y-axis. Thus, the current output remains unchanged if the mesh size is reduced indiscriminately without identifying the optimal meshing strategy. These findings emphasize the need for careful y-axis meshing in SOFC simulations to ensure reliable and precise predictions.

The importance of this finding lies in optimizing computational efficiency without compromising accuracy in SOFC CFD simulation. In identifying the y-axis as the most influential meshing parameter, researchers and engineers can more effectively allocate computational resources, guiding refinement where it will have the greatest impact. This information can be used to create more precise and computationally effective SOFC models, which will eventually enhance fuel cell design and optimization for practical use. Research in the future can be extended from here by further developing meshing techniques and their effects on various SOFC designs, increasing the predictive nature of CFD simulations in fuel cell research.

CONCLUSION

This study aimed to investigate the impact of mesh refinement on the accuracy of Computational Fluid Dynamics (CFD) simulations for Solid Oxide Fuel Cells (SOFCs), with a particular focus on the influence of y-axis meshing. The objective was to determine the optimal mesh size that ensures accurate current output predictions while maintaining computational efficiency. The methodology involved varying the number of elements and adjusting mesh sizes along different axes—x, y, and z—while analyzing the percentage difference in current output. The results demonstrated that refining the y-axis mesh significantly enhances accuracy, reducing percentage differences to below 5% when the mesh size is reduced to 1.50E-05 or smaller. However, further reductions beyond this threshold showed minimal improvements, indicating an optimal mesh resolution. Conversely, refining the x-axis and z-axis had negligible effects on accuracy, reinforcing the importance of targeted meshing strategies.

These findings provide valuable insights for optimizing SOFC simulations, ensuring both precision and computational efficiency. The study highlights the necessity of carefully selecting mesh sizes, particularly along the y-axis, where electrochemical reactions primarily occur. This understanding can be applied to real-world SOFC modeling and design, leading to more reliable performance predictions and improved fuel cell efficiency. For future research, it is recommended to explore the effects of mesh refinement on different SOFC geometries and operating conditions. Additionally, integrating advanced meshing techniques, such as adaptive meshing, could further enhance simulation accuracy while minimizing computational costs. These efforts will contribute to the advancement of SOFC technology, facilitating its adoption in clean energy applications.

ACKNOWLEDGEMENT

The authors would like to acknowledge funding from Ministry of Higher Education Malaysia, through High Education Center of Excellent (HiCoE) fund with code HICOE-2023-006 and also Research Grant (GP) with code GP-K017153. I would also like to acknowledge Universiti Kebangsaan Malaysia for providing facilities and expertise that greatly assisted this research

DECLARATION OF COMPETING INTEREST

None.

REFERENCES

Arifin, N. A., Afifi, A. A., Samreen, A., Hafriz, R. S. R. M. & Muchtar, A. 2023. Characteristic and challenges of scandia stabilized zirconia as solid oxide fuel cell material – In depth review. *Solid State Ionics* 399(116302.

Aznam, I., Muchtar, A., Somalu, M. R., Baharuddin, N. A. & Rosli, N. a. H. 2023. Advanced materials for heterogeneous catalysis: A comprehensive review of spinel materials for direct internal reforming of methane in solid oxide fuel cell. *Chemical Engineering Journal* 471(144751.

Chen, X., Ji, Y., Yang, J., Yan, D., Jia, L., Han, X., Wu, K. & Li, J. 2023. Flow uniformity analysis and optimization of a 60-cell external manifold solid oxide cell stack with bottom-accesses. *International Journal of Hydrogen Energy* 48(82): 32056-32067.

Ghorbani, B. & Vijayaraghavan, K. 2018. 3D and simplified pseudo-2D modeling of single cell of a high temperature solid oxide fuel cell to be used for online control strategies. *International Journal of Hydrogen Energy* 43(20): 9733-9748.

He, V., Gaffuri, M., Van Herle, J. & Schiffmann, J. 2023. Readiness evaluation of SOFC-MGT hybrid systems with carbon capture for distributed combined heat and power. *Energy Conversion and Management* 278(116728.

Khanafer, K., Al-Masri, A., Vafai, K. & Preethichandra, P. 2022. Heat up impact on thermal stresses in SOFC for mobile APU applications: Thermo-structural analysis. *Sustainable Energy Technologies and Assessments* 52(102159.

Lee, K. X., Hu, B., Dubey, P. K., Anisur, M. R., Belko, S., Aphale, A. N. & Singh, P. 2022. High-entropy alloy anode for direct internal steam reforming of methane in SOFC. *International Journal of Hydrogen Energy* 47(90): 38372-38385.

Mah, J. C. W., Aznam, I., Muchtar, A., Somalu, M. R. & Raharjo, J. 2023. Synthesis of (Cu,Mn,Co)3O4 Spinel: Effects of Citrate-to-Nitrate Ratio on Its Homogeneity and Electrical Properties. *Energies* 16(3): 1382.

Mathur, L., Namgung, Y., Kim, H. & Song, S.-J. 2023. Recent progress in electrolyte-supported solid oxide fuel cells: a review. *Journal of the Korean Ceramic Society* 60(4): 614-636.

Mehrabian, M. & Mahmoudimehr, J. 2023. A correlation for optimal steam-to-fuel ratio in a biogas-fueled solid oxide fuel cell with internal steam reforming by using Artificial Neural Networks. *Renewable Energy* 219(119397.

Mohd Abd Fatah, A. F., Rosli, A. Z., Mohamad, A. A., Muchtar, A., S.A., M. A. & Hamid, N. A. 2022. Electrochemical Evaluation of Nickel Oxide Addition toward Lanthanum Strontium Cobalt Ferrite Cathode for Intermediate Temperature Solid Oxide Fuel Cell (IT-SOFCS). *Energies* 15(14): 5188.

Muhammed Ali Shaikh Abdul Kader Abdul, H., Muchtar, A., Raharjo, J. & Khaerudini, D. S. 2022. A Review on the Process-Structure-Performance of Lanthanum Strontium Cobalt Ferrite Oxide for Solid Oxide Fuel Cells Cathodes. *International Journal of Integrated Engineering* 14(2): 121-137.

Nouri, F., Maghsoudy, S. & Habibzadeh, S. 2024. Dynamic insights of carbon management and performance enhancement approaches in biogas-fueled solid oxide fuel cells: A computational exploration. *International Journal of Hydrogen Energy* 50(1314-1328.

Pang, Z., Han, J., Feng, J., Diao, A., Yao, Y. & Peng, X. 2024. Performance prediction and geometry optimization of ejector in PEMFC system using coupled CFD-BPNN and genetic algorithm. *Applied Thermal Engineering* 251(123584.

Pongratz, G., Subotić, V., Hochenauer, C., Scharler, R. & Anca-Couce, A. 2022. Solid oxide fuel cell operation with biomass gasification product gases: Performance- and carbon deposition risk evaluation via a CFD modelling approach. *Energy* 244(123085.

Shieela Kalib, N., Muchtar, A., Zhen Yuan, V., Rao Somalu, M. & Kamal Ariffin Mohd Ihsan, A. 2022. Thermal Investigation of Solid Oxide Fuel Cell Ni-YSZ Anode supported with Cooling System: A FEM Approach. *IOP Conference Series: Materials Science and Engineering* 1257(1): 012019.

Singh, M., Zappa, D. & Comini, E. 2021. Solid oxide fuel cell: Decade of progress, future perspectives and challenges. *International Journal of Hydrogen Energy* 46(54): 27643-27674.

Tikiz, I., Taymaz, I. & Pehlivan, H. 2019. CFD modelling and experimental validation of cell performance in a 3-D planar SOFC. *International Journal of Hydrogen Energy* 44(29): 15441-15455.

Zainon, A. N., Somalu, M. R., Kamarul Bahrain, A. M., Muchtar, A., Baharuddin, N. A., S.A, M. A., Osman, N., Abdul Samat, A., Azad, A. K. & Brandon, N. P. 2023. Challenges in using perovskite-based anode materials for solid oxide fuel cells with various fuels: a review. *International Journal of Hydrogen Energy* 48(53): 20441-20464.

Zhang, X., Espinoza, M., Li, T. & Andersson, M. 2021. Parametric study for electrode microstructure influence on SOFC performance. *International Journal of Hydrogen Energy* 46(75): 37440-37459.